Steel and Composite Structures, *Vol. 18, No. 3 (2015) 757-773*
DOI: http://dx.doi.org/10.12989/scs.2015.18.3.757

Shear strength of steel beams with trapezoidal corrugated webs using regression analysis

Samer Barakat *, Ahmad Al Mansouri [a] and Salah Altoubat [b]

Department of Civil and Environmental Engineering, University of Sharjah, Sharjah, UAE

(*Received October 24, 2013, Revised August 08, 2014, Accepted September 26, 2014*)

Abstract. This work attempts to implement multiple regression analysis (MRA) for modeling and predicting the shear buckling strength of a steel beam with corrugated web. It was recognized from theoretical and experimental results that the shear buckling strength of a steel beam with corrugated web is complicated and affected by several parameters. A model that predicts the shear strength of a steel beam with corrugated web with reasonable accuracy was sought. To that end, a total of 93 experimental data points were collected from different sources. Then mathematical models for the key response parameter (shear buckling strength of a steel beam with corrugated web) were established via MRA in terms of different input geometric, loading and materials parameters. Results indicate that, with a minimal processing of data, MRA could accurately predict the shear buckling strength of a steel beam with corrugated web within a 95% confidence interval, having an R^2 value of 0.93 and passing the F- and t-tests.

Keywords: shear strength; steel beams; trapezoidal corrugated web; regression

1. Introduction

Steel beams with corrugated webs are a relatively recent development in structural systems and have seen a lot of use in bridge construction. They are typically composed of corrugated steel plates (forming the web) that are welded to a pair of flanges (Fig. 1).

The corrugations can take many shapes: rectangular, triangular, semi-circular, sinusoidal (as seen in Fig. 1), and trapezoidal (Fig. 2), the latter of which is the focus of this paper. Fig. 2(a) shows an example of a trapezoidal corrugated steel beam. Fig. 2(b) shows a cross-section through that beam and identifies all the relevant geometric properties for such a configuration: the length of the horizontal corrugation (a), the length of the horizontal projection of the diagonal corrugation (b), the length of the diagonal corrugation (c), the depth of the corrugation (d), the angle of corrugation (θ), and the thickness of the web (t_w).

Steel beams with corrugated webs have been shown theoretically and experimentally to have higher shear strength than beams with straight webs, alleviating the need for transverse stiffeners. A number of studies have been carried out to quantify this effect, attempting to express the

*Corresponding author, Professor, E-mail: sbarakat@sharjah.ac.ae
[a] M.Sc. Student, E-mail: ahmadalmansouri@gmail.com
[b] Associate Professor, E-mail: saltoubat@sharjah.ac.ae

Copyright © 2015 Techno-Press, Ltd.
http://www.techno-press.org/?journal=scs&subpage=8 ISSN: 1229-9367 (Print), 1598-6233 (Online)

Fig. 1 Corrugated steel plates being welded to flanges at Zeman International plant in Austria, forming corrugated web steel beams

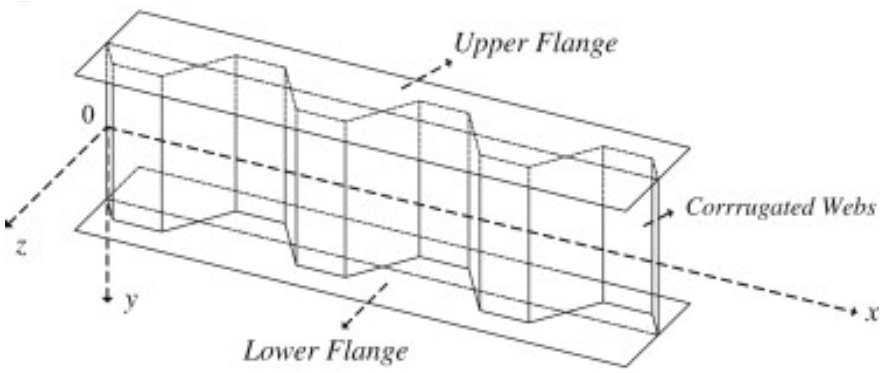

(a)

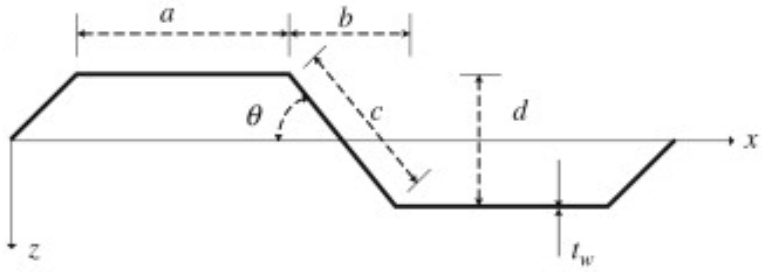

(b)

Fig. 2 I-girder with corrugated steel webs: (a) profile; (b) geometric notations (Moon *et al*. 2009)

increase in shear strength of the section in terms of the geometry of the corrugations and the material properties (see for example Abbas *et al*. 2002, 2006, Gil *et al*. 2005, Yi *et al*. 2008, Yong *et al*. 2013). Sause and Braxtan (2011) collected test results from eight different experiments on the shear strength of trapezoidal corrugated steel webs. Their objective was to test the accuracy of an equation proposed by an earlier researcher, El Metwally (1998), to calculate the shear stress

capacity of such sections and to modify this equation to better reflect the experimental results. All in all, they collected a total of 102 data points (see Appendix for a complete table of the results). However, because El Metwally's equation was derived from the local and global buckling theories, Sause and Braxtan (2011) could only use 22 of the 102 results in their study, as those were the only results originating from test conditions that were compatible with the assumptions of the theories. The motivation behind this paper is to find a more inclusive equation to calculate the shear buckling strength of beams with corrugated webs that would not be subject to the same restrictions. To that end, the approach of this paper will be to derive an equation from the test results themselves, setting aside a portion of the results to verify the accuracy of the equation. It should be noted that this paper will refer to the dimensions of the corrugated web using the notation defined in Sause and Braxtan (2011), which is shown in Fig. 3. It should also be noted that this notation is different to that of Fig. 2.

Two modes of shear buckling are defined: local and global buckling. Local buckling refers to deformations occurring in individual folds of the web. These deformations can occur simultaneously in multiple folds and can propagate into adjacent unaffected folds. Global buckling, on the other hand, occurs over several folds, the buckled shape extending diagonally over the depth of the web. Because of the similarity between global buckling and multiple simultaneous local buckling, experimentally observed buckling often appears to have characteristics of both modes. Local buckling is considered to be controlled by the slenderness of the individual folds of the webs, whereas global buckling is considered to be controlled by the slenderness of the entire web.

The local shear buckling stress of a corrugated web can be predicted using plate buckling theory. As described by Timoshenko and Gere (2009), a single fold of the web is considered to be supported along its horizontal edges by the flanges of the beam, and along its vertical edges by the adjacent folds. The local elastic shear buckling stress, $\tau_{L,el}$, can then be expressed as

$$\tau_{L,el} = k_L \frac{\pi^2 E}{12(1-\nu^2)(w/t_w)^2} \tag{1}$$

where k_L is a coefficient that depends on the aspect ratio of the folds and the boundary conditions of the beam, E is Young's modulus, ν is Poisson's ratio, w is the fold width, and t_w is the thickness of the web. Of these values, only w, the fold width, changes from fold to fold. For longitudinal folds, $w = b$ (Fig. 3), and for inclined folds, $w = c$. The larger of b and c is taken to determine the smallest value of $\tau_{L,el}$. As for k_L, it is smallest when the ratio of w/h_w is small (where h_w is the height of the web) and when the beam is simply supported, taking a value of 5.34. Fixed support raises this value to 8.98.

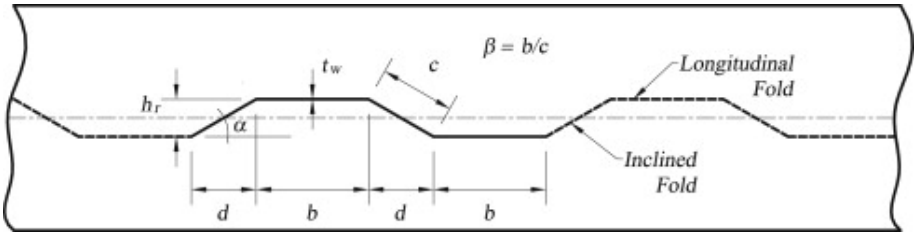

Fig. 3 Beam with corrugated web (section through web), Sause and Braxtan (2011)

Similarly, an expression for the global shear buckling stress for a corrugated plate can be derived from the orthotropic plate theory. Easley (1975) developed the following expression for the global shear buckling stress $\tau_{G,el}$

$$\tau_{G,el} = k_G \frac{(D_y)^{1/4} \cdot (D_x)^{3/4}}{t_w \cdot h_w^2} \tag{2}$$

where k_G is a coefficient that depends on the boundary conditions of the plate. It is minimized when the beam is long compared to h_w. Elgaaly *et al*. (1996) recommend taking k_G as 31.6, assuming the flanges simply support the web, or 59, assuming the web is fixed to the flanges. D_y and D_x are defined as follows

$$D_y = \frac{b+d}{b+d \cdot \sec(\alpha)} \cdot \frac{E \cdot t_w^3}{12} \tag{3}$$

$$D_x = \frac{E}{b+d}\left(\frac{b \cdot t_w \cdot (d \cdot \tan(\alpha))^2}{4} + \frac{t_w \cdot (d \cdot \tan(\alpha))^3}{12 \sin(\alpha)} \right) \tag{4}$$

where α is the angle of corrugation and d is the longitudinal projection of the inclined fold, as shown in Fig. 3.

In his Ph.D. Dissertation, Abbas combined Eqs. (2)-(4) to express the global shear buckling stress directly in terms of the geometric parameters shown in Fig. 3

$$\tau_{G,el} = k_G F(\alpha,\beta) \frac{E t_w^{1/2} b^{3/2}}{12 h_w^2} = C_G \frac{E t_w^{1/2} b^{3/2}}{12 h_w^2} \tag{5}$$

where $F(\alpha, \beta)$ is coefficient based on the dimensions of the corrugations of the web, defined as follows

$$F(\alpha,\beta) = \sqrt{\frac{1+\beta \sin^3 \alpha}{\beta + \cos\alpha}} \cdot \left\{ \frac{3\beta+1}{\beta^2(\beta+1)} \right\}^{3/4} \tag{6}$$

where β is the ratio of b to c. Most trapezoidal corrugated plates have a β value ranging between 1 and 2, Sause and Braxtan (2011). Any lower and the corrugations become too deep, requiring an uneconomical amount of material. Any higher and the corrugations become too shallow to contribute significantly to the shear buckling resistance of the plate. Similarly, the corrugation angle α usually ranges between 30° and 45°. Corrugation angles less than 30° render the folds of the web unable to fully support one another Linder and Hunag (1995).

It is possible that an interaction between local and global buckling modes exist. Past studies have attempted to illustrate this relationship and demonstrate its effect on both buckling modes using interaction formulas. One such formula, proposed by Linder and Aschinger (1988), can be expressed as follows

$$\frac{1}{(\tau_{I,el})^n} = \frac{1}{(\tau_{L,el})^n} + \frac{1}{(\tau_{G,el})^n} \tag{7}$$

where $\tau_{I,el}$ is the elastic shear buckling stress due to interaction and n is an integer. Yi *et al*. (2008)

proposed a formula based on Eq. (7) with $n = 1$. Solving for $\tau_{I,el}$, that formula becomes

$$\frac{1}{\tau_{I,n,el}} = \frac{\tau_{L,el} \cdot \tau_{G,el}}{((\tau_{L,el})^n \cdot (\tau_{G,el})^n)^{1/n}} \tag{8}$$

The local, global and interaction buckling slenderness ratios are defined as follows, respectively

$$\lambda_L = \sqrt{\frac{\tau_y}{\tau_{L,el}}} = \sqrt{\frac{12(1-\nu^2)\tau_y}{k_L \pi^2 E}} \frac{w}{t_w} \tag{9}$$

$$\lambda_G = \sqrt{\frac{\tau_y}{\tau_{G,el}}} = \sqrt{\frac{12\tau_y \cdot h_w^2}{k_G \cdot F(\alpha,\beta) \cdot E \cdot t_w^{1/2} \cdot b^{3/2}}} \tag{10}$$

$$\lambda_{I,n} = \sqrt{\frac{\tau_y}{\tau_{I,n,el}}} = \lambda_L \lambda_G \left(\left(\frac{1}{\lambda_L} \right)^{2n} + \left(\frac{1}{\lambda_G} \right)^{2n} \right)^{1/2n} \tag{11}$$

where the exponent n is an integer and τ_y is the shear yield stress according to the Von Mises yield criterion, defined as

$$\tau_y = \frac{F_y}{\sqrt{3}} \tag{12}$$

and F_y is the uniaxial yield stress of the web.

The normalized local, global, and interaction elastic shear buckling strengths can be determined from the slenderness ratios. They are, respectively

$$\rho_{L,el} = \frac{1}{\lambda_L^2} \tag{13}$$

$$\rho_{G,el} = \frac{1}{\lambda_G^2} \tag{14}$$

$$\rho_{I,n,el} = \frac{1}{\lambda_{I,n}^2} \tag{15}$$

It should be noted that all of the equations thus far have only considered elastic shear buckling stress. Elgaaly *et al*. (1996) provided an expression for the inelastic shear buckling stress

$$\tau_{inel} = \sqrt{0.8\tau_y \tau_{el}} \le \tau_y \tag{16}$$

Eq. (16) can be used in place of both $\tau_{el,L}$ or $\tau_{el,G}$ if either of them exceeds $0.8\tau_y$. The normalized inelastic shear buckling strength then becomes

$$\rho_{inel} = \frac{\tau_{inel}}{\tau_y} = \sqrt{\frac{0.8}{\lambda^2}} = \frac{0.8944}{\lambda} \le 1 \tag{17}$$

While the theories given above have been developed for corrugated webs in pure shear, they have been used to predict the shear buckling stress for steel I-beams under shear and flexure. Experiments conducted by Sause and Braxtan (2003) have shown that there is no significant contribution by corrugated webs to flexural strength. Therefore, the vertical shear stress in the web can be expressed as a constant average shear stress over the height of the web, calculated as follows

$$\tau = \frac{V}{h_w t_w} \tag{18}$$

where V is the vertical shear force in the beam. However, this expression ignores the shear stress in the flanges, which should be taken into account when interpreting experimental results.

El Metwally (1998) presents a formula based on the interaction theory for the shear strength of corrugated webs. It is applicable over the full range of behavior, including cases where inelastic buckling and yielding control.

$$\tau_{I,el} = \left(\frac{1}{(\tau_{L,el})^n} + \frac{1}{(\tau_{G,el})^n} \frac{1}{(\tau_y)^n} \right)^{-1/n} \tag{19}$$

where τ_n cannot exceed the minimum of $\tau_{L,el}$, $\tau_{G,el}$, τ_y, and n is an integer. El Metwally (1998) suggests using $n = 2$ for trapezoidal corrugations. Based on this equation, the normalized shear strength becomes

$$\rho_n = \frac{\tau_n}{\tau_y} = \left(\frac{1}{(\rho_{L,el})^n} + \frac{1}{(\rho_{G,el})^n} + 1 \right)^{-1/n} = \left(\frac{1}{\lambda_{I,n}^{2n} + 1} \right)^{1/n} \tag{20}$$

For trapezoidal corrugated webs, the equation becomes

$$\rho_n = \frac{\tau_n}{\tau_y} = \left(\frac{1}{(\rho_{L,el})^2} + \frac{1}{(\rho_{G,el})^2} + 1 \right)^{-1/2} = \left(\frac{1}{(\lambda_{I,2})^4 + 1} \right)^{1/2} \tag{21}$$

Sause and Braxtan (2011) suggest that a more accurate formula could be reached by replacing the 1 in Eq. (21) with a variable u and varying the exponent n. After comparing the results from several different versions of their formula to published test results, they conclude that $u = 2$ and $n = 3$ achieve the most accurate results. They also find this equation more accurate than those proposed by El Metwally (1998) and Yi *et al*. (2008).

$$\rho_{n,B} = \frac{\tau_{n,B}}{\tau_y} = \left(\frac{1}{(\rho_{L,el})^3} + \frac{1}{(\rho_{G,el})^3} + 2 \right)^{-1/3} = \left(\frac{1}{(\lambda_{I,3})^6 + 2} \right)^{1/3} \tag{22}$$

2. Multiple Regression Analysis (MRA)

2.1 Scatter plots

To acquire an overall perspective of the inherent relationships of the problem, the pairs of the

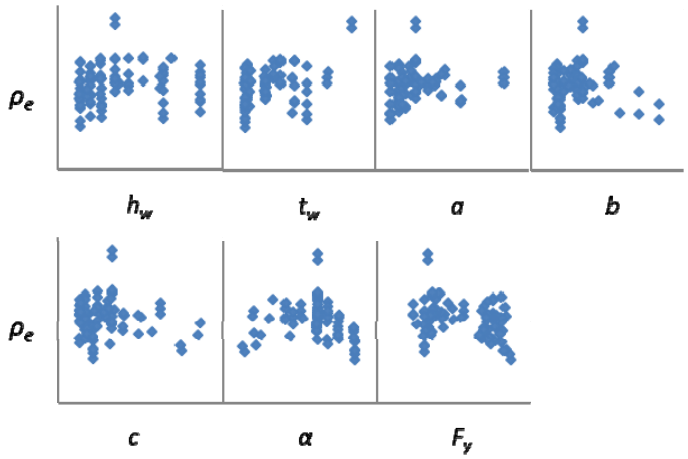

Fig. 4 Comparison between pairs of variables of interest

variables of interest are examined in the matrix scatter diagram shown in Fig. 4. From left to right they are: the height of the web h_w, the thickness of the web t_w, the shear span a, the length of longitudinal fold b, the length of inclined fold c, the angle of corrugation α, the uniaxial yield stress of the web F_y, and the experimental normalized shear buckling strength ρ_e. In an effort to capture the simplest form of relationships via regression, linear relationships are investigated first in the MRA. Subsequently, nonlinear components are explicitly allowed in the formulation (Ang and Tang 2007).

2.2 Linear regression models

In a simple regression model, the constant represents the Y-intercept of the regression line. On the other hand, in a multiple regression model, the constant represents the value that would be predicted for the dependent variable if all the independent variables were simultaneously equal to zero. Out of the 102 data points, 8 are omitted because their shear span, a, was not reported. Each of the 93 remaining data points is randomly assigned to one of two sets. 73 data points are assigned to set 1, from which the linear regression model is to be derived. 20 data points are assigned to set 2, against which the results of the linear regression model are to be checked. The linear regression model between the dependent variable (ρ_e) and the all independent variables (h_w, t_w, a, b, c, α, F_y) is then calculated using data set 1.

Table 1 summarizes the (SPSS, Inc. 2010) outputs for the ρ_e model. The terms included in this table to explain the overall model fit in the regression analysis are:

- R^2: The proportion of variance in the dependent variable ρ_e which can be explained by the independent variables. This is an overall measure of the strength of association and does not reflect the extent to which any particular independent variable is associated with the dependent variable. The adjusted R^2 value is an adjustment of the R^2 value that penalizes the addition of extraneous predictors to the model. The adjusted R^2 value is given by $1 - ((1 - R^2)(N - 1) / (N - k - 1))$, where k is the number of predictors and N is the number of data points.
- F-value and F-significance: The F-statistic the p-value associated with it. The F-statistic is

Table 1 Linear regression results

R^2	F-value		F-significance
0.965	258.882		0
Variable	**Coefficient**	**t-value**	**t-significance**
h_w	0.000	2.087	0.41
a	–2.087E–005	–0.412	0.682
t_w	0.105	5.042	0.000
b	0.002	1.764	0.082
α	0.009	4.304	0.000
c	-0.003	–2.393	0.020
F_y	0.000	1.310	0.195

the mean square (regression) divided by the mean square (residual). The p-value is compared to some alpha level in testing the null hypothesis that all of the model coefficients are 0.

- Coefficient t-value and t-significance: The t-statistics and their associated 2-tailed p-values used in testing whether a given coefficient is significantly different from zero using an alpha of 0.05.

The multiple regression model does not include constant terms. Consequently, if all the independent variables take the value of zero simultaneously, the dependent variables will also be equal to zero. This is in agreement with the modeled physical phenomenon.

Despite the apparent good-fitting and passing the F-test, the linear model is deemed physically unsound for the ρ_e prediction. This is attributed to the negative signs on two of the independent variables coefficients, and the negligibly small coefficients of two others. For example, this implies that increasing the shear span (a) or the length of the diagonal fold (c) decreases ρ_e and that changing the yield stress (F_y) doesn't change ρ_e, which is counterintuitive. Moreover, two coefficients (those of α and c) fail the t-test. Consequently, nonlinear regression models are reverted to.

2.3 Nonlinear regression models

Nonlinear regression is appropriate when the relationship between the dependent and independent variables is not intrinsically linear. Nonlinear regression can estimate models with arbitrary relationships between independent and dependent variables. The relationship of the dependent variable ρ_e in terms of each of the independent variables is generally non-flat. Therefore, new nonlinear functions are created from the original variables in the original data set (El-Shaarawi and Walter 2002). These new variables are created in forms that guarantee that the curved functions of the original variables are transformed to linear functions of the new variables. This is described by Eqs. (23)-(24)

$$Y = a_1 f_i \tag{23}$$

$$f_i = g_i(\ldots) \tag{24}$$

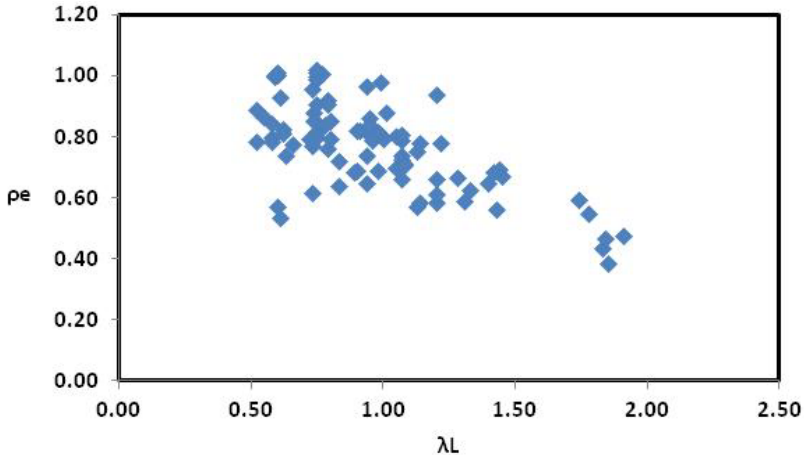

Fig. 5 Normalized shear buckling strength ρ_e vs. local slenderness ratio λ_L

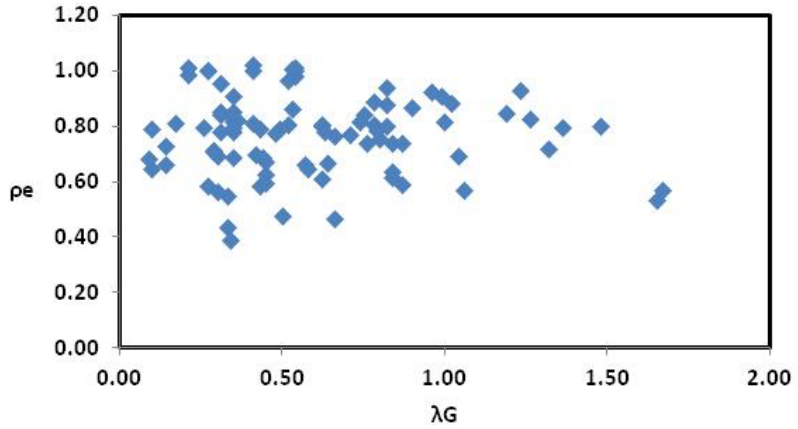

Fig. 6 Normalized shear buckling strength ρ_e vs. global slenderness ratio λ_G

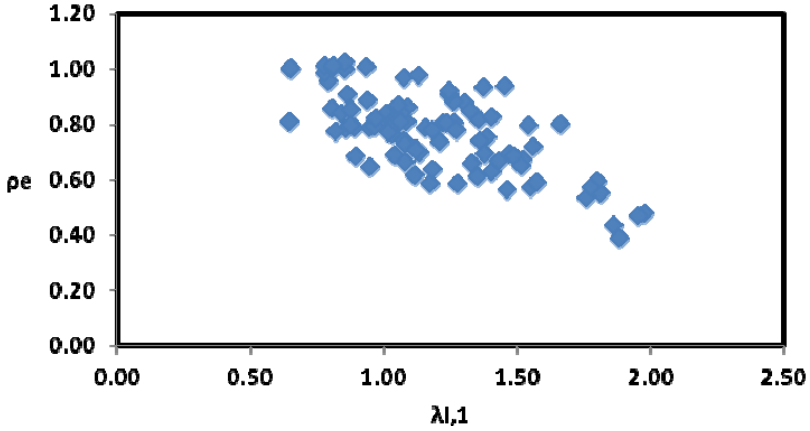

Fig. 7 Normalized shear buckling strength ρ_e vs. interactive slenderness ratio λ_I

Table 2 Nonlinear regression results

R^2	F-value	F-significance
0.930	956.704	0

Variable	Coefficient	t-value	t-significance
$1 / \lambda_{I,1}$	0.747	30.931	0

Table 3 Effect of exponent n on accuracy

n	R^2
1	0.930
2	0.921
3	0.916
4	0.913
5	0.913

where Y represents the dependent variable ρ_e. A careful selection of the function f_i in Eq. (24) results in a linear relationship in Eq. (23), in which the constant a_1 can be estimated using traditional linear regression procedures. To find the transformation functions g_i, different nonlinear models are considered. Based on several trials of functions that preserve the physical interpretation, many transformation functions were obtained. Noting the aforementioned relationship between the slenderness ratios and the theoretical normalized shear buckling strengths (see Eqs. (13)-(15)), it was proposed that there could similarly be good correlation between the slenderness ratios and the shear buckling strength derived from the experimental results. In order to investigate this potential relationship the experimental normalized shear buckling strength ρ_e was plotted against each of the slenderness ratios (Figs. 5-7).

The distribution of data points in Fig. 7 indicates a significant inversely proportional relationship between ρ_e and $\lambda_{I,1}$ (Eq. (11) with $n = 1$). Performing linear regression between ρ_e and $1 / \lambda_{I,1}$ confirms this relationship, producing an R^2 value of 0.934, as well as passing the F- and t-tests (see Table 2).

The effect of the exponent n on this relationship was explored by performing linear regression again between ρ_e and $1 / \lambda_{I,1}$ where n was every integer between 1 and 5. The results are summarized in Table 3. It is clear that R^2 value is the highest for $n = 1$. Therefore, the best discovered regression model is as follows

$$\rho_e = \frac{0.747}{\lambda_{I,1}} \tag{25}$$

where

$$\lambda_{I,1} = \lambda_L \lambda_G \sqrt{\left(\left(\frac{1}{\lambda_L}\right)^2 + \left(\frac{1}{\lambda_G}\right)^2\right)} \tag{26}$$

and λ_L and λ_G are as in Eqs. (9) and (10), respectively.

The accuracy of the regression models was checked. The input values from set 1 of data were presented to the MRA model to perform the necessary calculations and produce the corresponding

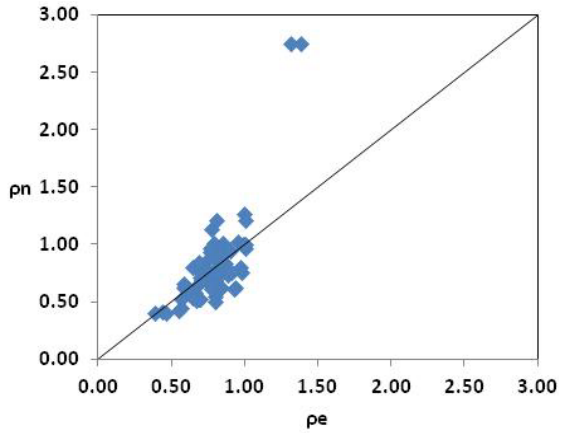

Fig. 8 Set 1's recalled normalized shear buckling strength ρ_n vs. experimental ρ_e

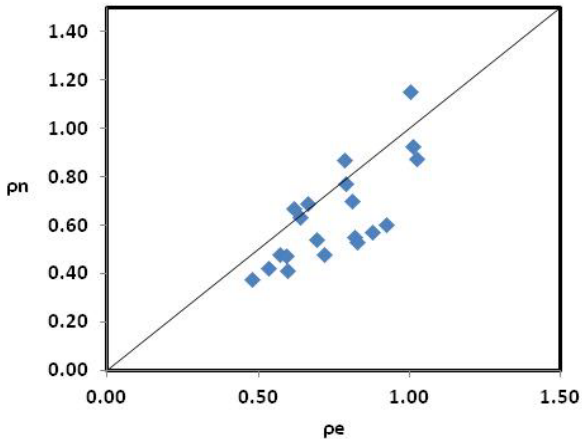

Fig. 9 Set 2's predicted normalized shear buckling strength ρ_n vs. experimental ρ_e

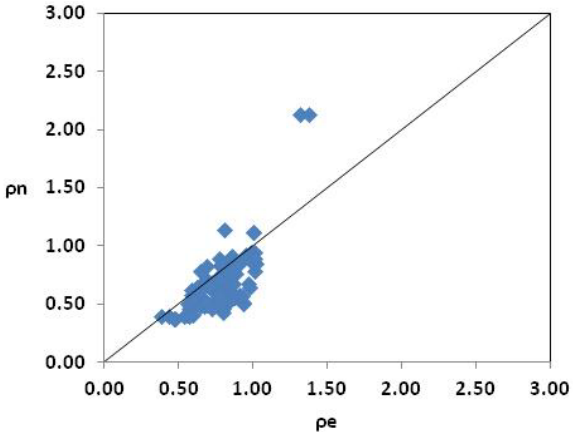

Fig. 10 Combined predicted normalized shear buckling ρ_n strength vs. experimental ρ_e

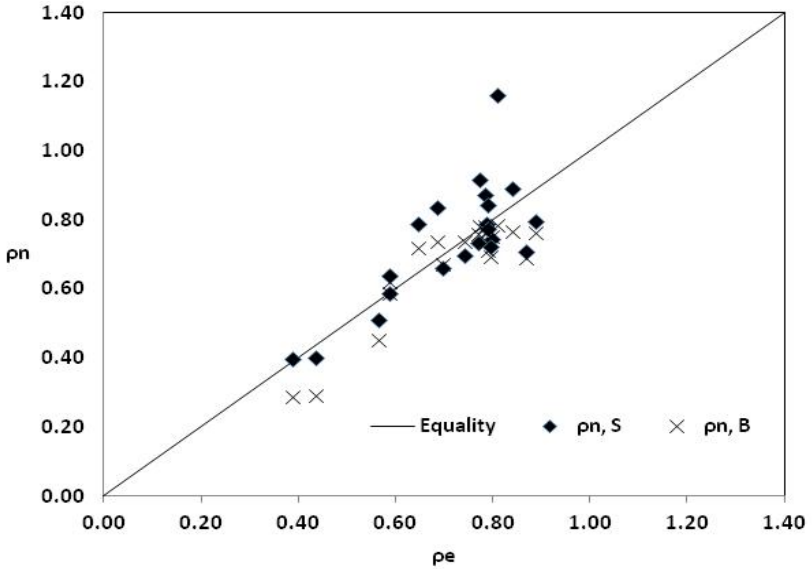

Fig. 11 Comparison between ρ_e, $\rho_{n,B}$ and $\rho_{n,S}$

outputs. Comparison of experimental values and predicted values of the shear buckling strength of a steel beam with corrugated web by MRA are presented in Fig. 8.

Furthermore, the prediction accuracy of the model adopted in this work was also checked. One additional set 2 of data consisting of 20 points were used to perform the prediction test using the MRA model. It should be stressed that all of the data in this later set was initially withheld from the MRA. The results of this test are shown in Fig. 9. The closeness of the points to the equality line serves only to indicate the validity of the MRA model. A comparison between the predicted values of all 93 specimens is shown in Fig. 10. Since most of the point lie beneath the equality line, it's determined that the MRA model has a tendency to underestimate the normalized shear buckling strength of a section. Nevertheless, there is a clear trend between the predicted and experimental values.

Fig. 11 shows a comparison between the normalized experimental shear buckling strength (ρ_e) of the 22 specimens that Sause and Braxtan (2011) focused their study on, their corresponding predicted normalized shear buckling strength ($\rho_{n,B}$), and the corresponding normalized shear buckling strength of the MRA model ($\rho_{n,S}$). Compared to Sause and Braxtan's (2011) model, the MRA model is a bit more dispersed, but it has the advantage of being applicable to a much wider range of sections and loading configurations.

3. Conclusions

This work aimed at studying the shear buckling strength of a steel beam with corrugated web. The theoretical and experimental results showed that the shear buckling strength of a steel beam with corrugated web is complicated and affected by several parameters. A simple model that predicts the shear strength of a steel beam with corrugated web with reasonable accuracy was sought. To that end, a total of 93 experimental data points were collected from different sources

and randomly assigned to one of two sets. 73 data points are assigned to set 1 for model derivation. 20 data points are assigned to set 2 for model checking. Then mathematical models for the key response parameter (shear buckling strength of a steel beam with corrugated web) were established via MRA in terms of different input geometric, loading and materials parameters. A number of different models were tested before settling on one that produced satisfactory results. The final model had an $\boldsymbol{R^2}$ value of **0.93** and passed the F- and t-tests. With this model, it is possible to predict the shear buckling strength of corrugated web sections from their geometric and material properties with good accuracy.

Acknowledgments

The research described in this paper is based upon work financially supported by the College of Graduate Studies and Research and the Research Department under the Office of the Vice Chancellor of Research and Graduate Studies (Grant No. 2014), University of Sharjah, Sharjah, UAE. This support is gratefully acknowledged.

References

Abbas, H.H., Sause, R. and Driver, R.G. (2002), "Shear strength and stability of high performance steel corrugated web girders", *Proceedings of Structural Stability Research Council Annual Technical Session*, Seattle, WA, USA, April, pp. 361-387.

Abbas, H.H., Sause, R. and Driver, R.G. (2006), "Behavior of corrugated web I-girders under in-plane loading", *J. Struct. Eng., ASCE*, **132**(8), 806-814.

Ang, A.H.S. and Tang, W.H. (2007), *Probability Concepts in Engineering: Emphasis on Applications to Civil and Environmental Engineering*, (2nd Ed.), John Wiley & Sons, New York, NY, USA.

Easley, J.T. (1975), "Buckling formulas for corrugated metal shear diaphragms", *J. Struct. Div.*, **101**(7), 1403-1417.

El Metwally, A.S. (1998), "Prestressed composite girders with corrugated steel webs", University of Calgary, Calgary, AB, Canada.

El-Shaarawi, A. and Walter, P. (2002), "Nonlinear regression, Gordon K. Smyth", In: Encyclopedia of Environmetrics, (ISBN 0471 899976), (Volume 3), John Wiley & Sons, Ltd., Chichester, UK, pp. 1405-1411.

Elgaaly, M., Hamilton, R.W. and Seshadri, A. (1996), "Shear strength of beams with corrugated webs", *J. Struct. Eng.*, **122**(4), 390-398.

Gil, H., Lee, S., Lee, J. and Lee, H.E. (2005), "Shear buckling strength of trapezoidally corrugated steel webs for bridges", *J. Transp. Res. Board*, Special Volume CD11-S, 473-480.

Linder, J. and Aschinger, T.R. (1988), "Grenzschubtragfähigkeit von I-Trägern mit trapezförmig profilierten Stäben", *Stahlbau*, **57**(12), 377-380.

Lindner, J. and Hunag, B. (1995), "Beulwerte für trapezförmig profilierte Bleche unter Schubbeanspruchung", *Stahlbau*, **64**(2), 370-374.

Moon, J., Yi, J., Choi, B.H. and Lee, H.E. (2008), "Lateral torsional buckling of I-girder with corrugated webs under uniform bending", *Thin-Wall. Struct.*, **47**(1), 21-30.

Moon, J., Yi, J., Choi, B.H. and Lee, H.-E. (2009), "Shear strength and design of trapezoidally corrugated steel webs", *J. Construct. Steel Res.*, **65**(5), 1198-1205.

Sause, R. and Braxtan, T.N. (2011), "Shear strength of trapezoidal corrugated steel webs", *J. Construct. Steel Res.*, **67**(2), 223-236.

Sause, R., Abbas, H.H., Wassef, W., Driver, R. and Elgaaly, M. (2003), "Corrugated web girder shape and

strength criteria", In: Work area 1, Pennsylvania innovative high performance steel bridge demonstration project, Bethlehem, PA, USA, *ATLSS Engineering Research Center*, Lehigh University, Bethlehem, PA, USA.

SPSS, Inc. (2010), SPSS ver. 19.0; Reference Manual, Chicago, IL, USA.

Timoshenko, S.P. and Gere, J.M. (2009), *Theory of Elastic Stability* (*Dover Civil and Mechanical Engineering*), Dover Publications, New York, NY, USA.

Yi, J., Gil, H., Youm, K. and Lee, H. (2008), "Interactive shear buckling behavior of trapezoidally corrugated steel webs", *Eng. Struct.*, **30**(6), 1659-1666.

Yong, D., Kebin, J., Fei, S. and Anzhong, D. (2013), "Experimental study on ultimate torsional strength of PC composite box-girder with corrugated steel Webs under pure torsion", *Struct. Eng. Mech., Int. J.*, **46**(4), 519-531.

CC

Appendix A: Experimental results collected by Sause and Braxtan (2011)

Specimen	h_w (mm)	t_w (mm)	a / h_w	b (mm)	β	d (mm)	α (°)	F_y (MPa)	ρ_e (τ_e / τ_y)
V-PILOTA	305	0.78	1.00	38.1	1.06	25.4	45.0	621	0.968
V-PILOTB	305	0.79	1.00	38.1	1.06	25.4	45.0	638	0.808
V121216A	305	0.64	1.00	38.1	1.06	25.4	45.0	676	0.660
V121216B	305	0.77	1.00	38.1	1.06	25.4	45.0	665	0.979
V181216B	457	0.61	0.67	38.1	1.06	25.4	45.0	618	0.939
V181216C	457	0.76	0.67	38.1	1.06	25.4	45.0	679	0.878
V181816A	457	0.64	1.00	38.1	1.06	25.4	45.0	591	0.754
V181816B	457	0.74	1.00	38.1	1.06	25.4	45.0	614	0.806
V241216A	610	0.64	0.50	38.1	1.06	25.4	45.0	591	0.572
V241216B	610	0.79	0.50	38.1	1.06	25.4	45.0	588	0.819
V121221A	305	0.63	1.00	41.9	1.03	23.4	55.0	665	0.627
V121221B	305	0.79	1.00	41.9	1.03	23.4	55.0	665	0.789
V122421A	305	0.68	2.00	41.9	1.03	23.4	55.0	621	0.587
V122421B	305	0.78	2.00	41.9	1.03	23.4	55.0	638	0.697
V181221A	457	0.61	0.67	41.9	1.03	23.4	55.0	578	0.665
V181221B	457	0.76	0.67	41.9	1.03	23.4	55.0	606	0.803
V181821A	457	0.64	1.00	41.9	1.03	23.4	55.0	552	0.611
V181821B	457	0.74	1.00	41.9	1.03	23.4	55.0	596	0.806
V241221A	610	0.61	0.50	41.9	1.03	23.4	55.0	610	0.591
V241221B	610	0.76	0.50	41.9	1.03	23.4	55.0	639	0.740
V121232A	305	0.64	1.00	49.8	0.87	26.4	62.5	665	0.549
V121232B	305	0.78	1.00	49.8	0.87	26.4	62.5	641	0.695
V121832A	305	0.64	1.50	49.8	0.87	26.4	62.5	703	0.435
V121832B	305	0.92	1.50	49.8	0.87	26.4	62.5	562	0.587
V122432A	305	0.64	2.00	49.8	0.87	26.4	62.5	714	0.387
V122432B	305	0.78	2.00	49.8	0.87	26.4	62.5	634	0.564
V181232A	457	0.60	0.67	49.8	0.87	26.4	62.5	552	0.594
V181232B	457	0.75	0.67	49.8	0.87	26.4	62.5	602	0.672
V181832A	457	0.61	1.00	49.8	0.87	26.4	62.5	689	0.477
V181832B	457	0.75	1.00	49.8	0.87	26.4	62.5	580	0.686
V241232A	610	0.62	0.50	49.8	0.87	26.4	62.5	673	0.468
V241232B	610	0.76	0.50	49.8	0.87	26.4	62.5	584	0.648
V121809A	305	0.71	1.50	19.8	1.07	11.9	50.0	572	0.888
V121809C	305	0.63	1.50	19.8	1.07	11.9	50.0	669	0.741
V122409A	305	0.71	2.00	19.8	1.07	11.9	50.0	586	0.786
V122409C	305	0.66	2.00	19.8	1.07	11.9	50.0	621	0.799
V181209A	457	0.56	0.67	19.8	1.07	11.9	50.0	689	0.796
V181209C	457	0.61	0.67	19.8	1.07	11.9	50.0	592	0.932

Specimen	h_w (mm)	t_w (mm)	a / h_w	b (mm)	β	d (mm)	α (°)	F_y (MPa)	ρ_e (τ_e / τ_y)
V181809A	457	0.61	1.00	19.8	1.07	11.9	50.0	618	0.827
V181809C	457	0.62	1.00	19.8	1.07	11.9	50.0	559	0.846
V241209A	610	0.62	0.50	19.8	1.07	11.9	50.0	606	0.533
V241209C	610	0.64	0.50	19.8	1.07	11.9	50.0	621	0.572
L1A	994	1.94	0.98	140	1.98	50	45.0	292	0.861
L1B	994	2.59	0.99	140	1.98	50	45.0	335	1.008
L2A	1445	1.94	1.04	140	1.98	50	45.0	282	0.738
L2B	1445	2.54	1.04	140	1.98	50	45.0	317	0.840
L3A	2005	2.01	1.00	140	1.98	50	45.0	280	0.691
L3B	2005	2.53	1.00	140	1.98	50	45.0	300	0.882
B1	600	2.10	1.33	140	1.98	50	45.0	341	0.838
B4	600	2.11	1.33	140	1.98	50	45.0	363	0.690
B4b	600	2.11	1.33	140	1.98	50	45.0	363	0.818
B3	600	2.62	1.33	140	1.98	50	45.0	317	0.855
B2	600	2.62	1.17	140	1.98	50	45.0	315	0.955
M101	600	0.99	1.00	70	3.30	15	45.0	189	0.818
M102	800	0.99	1.00	70	3.30	15	45.0	190	0.909
M103	1000	0.95	1.00	70	3.30	15	45.0	213	0.719
M104	1200	0.99	1.00	70	3.30	15	45.0	189	0.802
L1	1000	2.10	1.50	106	1.06	86.6	30.0	410	0.764
L1	1000	3.00	1.49	106	1.06	86.6	30.0	450	0.783
L2	1498	2.00	1.44	106	1.06	86.6	30.0	376	0.923
L2	1498	3.00	1.43	106	1.06	86.6	30.0	402	0.868
No. 1	850	2.00	1.33	102	1.00	85.5	33.0	355	0.789
No. 2	850	2.00	1.33	91	1.00	71.5	38.2	349	0.774
V1/1	298	2.05	9.46	144	1.00	102	45.0	298	0.647
V1/2	298	2.10	6.71	144	1.00	102	45.0	283	0.685
V1/3	298	2.00	3.36	144	1.00	102	45.0	298	0.790
V2/3	600	3.00	2.75	144	1.00	102	45.0	279	0.810
SP1	800	2.00	2.19	146	0.99	104	45.0	307	0.795
SP2	800	2.00	2.19	170	1.50	80	45.0	299	0.781
SP3	800	2.00	2.19	185	2.01	65	45.0	292	0.778
SP4	800	2.00	2.25	117	1.00	83	45.0	298	0.840
SP5	800	2.00	2.25	136	1.50	64	45.0	291	0.822
SP6	800	2.00	2.25	148	2.01	52	45.0	294	0.811
SP2-2-400 1	400	2.00	2.50	170	1.50	80	45.0	263	0.662
SP2-2-400 2	400	2.00	2.50	170	1.50	80	45.0	263	0.727
SP2-2-800 1	800	2.00	1.25	170	1.50	80	45.0	272	0.712
SP2-2-800 2	800	2.00	1.25	170	1.50	80	45.0	272	0.707
SP2-3-600 1	600	3.00	1.67	170	1.50	80	45.0	294	0.987

Specimen	h_w (mm)	t_w (mm)	a / h_w	b (mm)	β	d (mm)	α (°)	F_y (MPa)	ρ_e (τ_e / τ_y)
SP2-3-600 2	600	3.00	1.67	170	1.50	80	45.0	294	1.010
SP2-3-1200 1	1200	3.00	0.83	170	1.50	80	45.0	294	1.000
SP2-3-1200 2	1200	3.00	0.83	170	1.50	80	45.0	294	1.023
SP2-4-800 1	800	4.00	1.25	170	1.50	80	45.0	326	1.000
SP2-4-800 2	800	4.00	1.25	170	1.50	80	45.0	326	1.003
SP2-4-1600 1	1600	4.00	0.63	170	1.50	80	45.0	328	1.003
SP2-4-1600 2	1600	4.00	0.63	170	1.50	80	45.0	328	1.012
SP2-8-800 1	800	8.00	1.25	170	1.50	80	45.0	270	1.314
SP2-8-800 2	800	8.00	1.25	170	1.50	80	45.0	270	1.381
L1	1500	4.80	NA	450	1.25	300	33.7	250	0.719
L2	1500	4.80	NA	550	1.55	300	32.2	250	0.603
L3	1500	4.80	NA	450	1.48	300	9.4	250	0.513
L4	1500	4.80	NA	550	1.80	300	10.6	250	0.457
I1	2000	4.80	NA	320	2.92	100	24.0	250	0.950
I2	2000	3.80	NA	350	3.37	100	16.0	250	0.517
G1	2000	4.80	NA	200	1.08	180	14.2	250	0.793
G2	2000	3.80	NA	160	2.67	50	33.4	250	0.834
G3	2000	3.80	NA	160	1.55	100	15.1	250	0.850
G8A	1500	6.27	3.00	300	1.20	200	36.9	465	0.853
G7A	1500	6.30	3.00	300	1.20	200	36.9	465	0.907
SC1	1500	6.27	3.00	300	1.20	200	36.9	465	0.796
MI2	2000	4.00	1.40	250	1.10	220	15.3	296	0.639
MI3	2000	4.00	1.40	220	1.16	180	18.4	296	0.617
MI4	2000	4.00	1.40	220	1.13	180	22.6	296	0.770